Journal of Macromolecular Science®, Part C: Polymer Reviews, 45:289–308, 2005

ISSN 1532-1797 print/1532-9038 online
DOI: 10.1080/15321790500304098

Taylor & Francis
Taylor & Francis Group

Focused Review

The Influence of Chemical Structure on Polyolefin Melt Rheology and Miscibility

DAVID J. LOHSE

Corporate Strategic Research, ExxonMobil Research and Engineering Co., Annandale, NJ, USA

The ability to predict polymer properties from a knowledge of the chemical architecture of the chains is one of the main goals of polymer science, and achievement of this can be very useful in the development of new polymeric materials. In this paper the connection between dimensions of polyolefin chains and some of their most fundamental properties, such as the degree of entanglement and miscibility, are described. The experimental and theoretical justifications of these relations are outlined in the first sections, and then the ways these can be used to predict the performance of polyolefins are demonstrated. Finally, other areas where such connections may be found in the future are suggested.

Keywords chemical architecture, polyolefin chains, rheology, miscibility, entanglement

Introduction

The chief way in which flexible polymers differ from other chemical substances is that they are so long that, in order to fill the available space, the individual molecules overlap with each other, that is, that they entangle (1). This entangled state is fundamentally responsible for the properties that distinguish polymers from other materials: their extremely slow dynamics (as seen in diffusion and viscosity), the fact that they are generally in a non-equilibrium state (e.g., semi-crystallinity), their mechanical performance (e.g., viscoelasticity), and so on. In fact, a common definition of the transition from "oligomers" to "polymers" is the molecular weight at which the chains begin to entangle. Thus, in order to see how polymer properties are related to their chemical makeup and so control the performance of polymeric materials, one needs to understand how the state of entanglement is determined by the chemical architecture of the chains.

Received 4 April 2005; Accepted 1 June 2005.
Address correspondence to David J. Lohse, Corporate Strategic Research, ExxonMobil Research and Engineering Co., Annandale, NJ 08801, USA. Tel.: 908-730-2541; Fax: 262-313-4775; E-mail: david.j.lohse@exxonmobil.com

In recent years, it has become apparent that the entangled nature of polymers is due to the fact that there are two measures of how "large" polymer coils are in the liquid or melt state (2–8). One of these is just the volume "occupied" by each chain, that is, the total volume divided by the number of molecules. The other is some measure of the extent of the space "pervaded" by the polymer chain. This can be related to the radius of the smallest sphere to totally enclose the chain (called the "span" of the chain) (9), the distance between the chain ends, R, or the radius of gyration of the chain, r_g. For small molecules, such as methane or *n*-hexane, the occupied and pervaded volumes are the same. The advent of small angle neutron scattering in the 1970s confirmed Flory's hypothesis that, when the chains are long enough, the pervaded volume is much larger than the occupied one (10). The part of the pervaded volume that is not occupied by the chain itself is occupied by other molecules, which gives rise to the state of entanglement (due to the fact that covalent chains cannot cross each other). The ability to relate chain dimensions to chemical structures will then allow one to predict how performance can be derived from the chemistry. This provides the roadmap to realizing the vision expressed by Flory in his text: "*Comprehension of the configurational statistics of chain molecules is indispensable for a rational interpretation and understanding of their properties"* (11).

In this review, I show how a great deal of progress has been made towards this goal, especially for the class of saturated hydrocarbon polymers commonly called polyolefins (12). Most of these are indeed products of the polymerization of one or more olefin, such as polyethylene (PE), polyisobutylene (PIB), polypropylene (PP), and their copolymers. But herein the term "polyolefins" is used more broadly to refer to all polymers that are built up from just hydrogen and carbon, and for which all of the covalent bonds are saturated. For instance, much of the work that has led to the results discussed here was done on hydrogenated polydienes (such as polybutadiene), which have structures identical to various olefin-derived polymers (13, 14). Indeed, since the goal is to relate properties to chemical structure, it does not matter how this architecture was synthesized, just the final result.

The interest in polyolefins has two sources. One is simply the practical importance of these materials, which are the largest class of synthetic polymers. More than 60 million metric tons are produced each year worldwide (12), or more than 10 kg for each citizen of the planet! Moreover, because of the great utility of these materials their use continues to grow on the order of 5% per year. So methods to improve the control of their performance will clearly be highly beneficial to society. Beyond this, advances in synthetic chemistry allow a wide range of saturated hydrocarbon polymers to be made with a great deal of control over the architecture. By saturating anionically synthesized polydienes, many well-defined polyolefin models can be made. Moreover, increasingly more sophisticated control of polyolefin structure is possible through metallocene (15) and metathesis (16) chemistries. These polymerization methods make it possible to study architecture-property relations in polyolefins much more deeply than for other polymer systems, and thus polyolefins can be used as models for all flexible polymers in this general program.

The focus of this review is to show that the objective of relating molecular structure to properties has now largely been realized in two areas for polyolefins: rheology and miscibility. In the first section the packing length model for entanglement[6] is described, and the way this can be used to predict various rheological parameters from a knowledge of chain size is shown. The second section outlines how the packing length can also be correlated to polyolefin miscibility (17, 18), and so the prediction of this critical property for the majority of blends. I finish with an outline of what remains to be done, particularly in the challenging area of predicting chain dimensions directly from chemical architecture.

Melt Rheology

Packing Length Model

A number of authors have developed models that relate the degree of entanglement of a polymer to the size of its chains (2–8), and the reader is directed to these papers for more details. Here I give some of the main results of this work, which shows how the molecular weight between entanglements, M_e, and the plateau modulus, G_N^0, are related to a quantity called the packing length (19).

The packing length can be derived from a comparison of the occupied and pervaded volumes of a chain, and arises naturally in theories of polymer blend interfaces (20) and block copolymers (19), as well as entanglements and rheology (6). Consider first the occupied volume, V_{occ}, which again is simply the volume per polymer molecule. This can be directly determined from the polymer density, ρ, Avogadro's number, N_A, and the molecular weight of the chain, M:

$$V_{occ} = \frac{M}{\rho N_A} \tag{1}$$

As stated above, the volume that is pervaded by a polymer chain is related to a measure of the chain size such as its radius of gyration, r_g, or the distance between the chain ends, R. The Flory hypothesis that polymer chains in the melt have the dimensions of ideal chains is now well confirmed by experimental evidence (10, 11). This means that the average of r_g^2 is proportional to M (in the limit of large M):

$$r_g^2 = KM \tag{2}$$

The value of K depends on temperature and the chemical structure of the polymer, which control factors such as the probability of *trans* vs. *gauche* rotations of the backbone bonds. Moreover, $R^2 = 6r_g^2$. Since both V_{occ} and r_g^2 are proportional to M, their ratio is a parameter independent of molecular weight and thus is a constant characteristic of the chemical structure of the polymer. This is called the packing length, l_p:

$$l_p = \frac{V_{occ}}{r_g^2} = \frac{M}{r_g^2 \rho N_A} \tag{3}$$

In previous work I have used a definition (19) of packing length based on R^2,

$$p = \frac{M}{R^2 \rho N_A} \tag{4}$$

Clearly, $l_p = 6p$. Herein I have adopted the use of l_p, which was first defined by Graessley (21), for two main reasons. First, r_g is the quantity actually measured by scattering experiments (10). Secondly, as will be seen below, the relations between l_p and M_e or G_N^0 have more natural units than those with p, having numerical coefficients of order 1.

The packing length is directly related to the statistical segment length of a polymer, b (11). This quantity is also related to the size of the chain and is given by

$$b^2 = 6r_g^2 \frac{m_0}{M} = \frac{6r_g^2 N_A \rho v_0}{M} = \frac{6v_0}{l_p} \tag{5}$$

where m_0 is the molecular weight of a monomer repeat unit, and v_0 its volume. Note that the definition of b requires the specification of a repeat unit, which is often problematic,

especially for copolymers. Moreover, when comparing a number of different polymers, one needs to define a constant value of v_0 as a reference volume, meaning that it will be arbitrary and so have no relation to the structure of the polymers. (Here I use a value of $v_0 = 0.1\,\text{nm}^3$.) For this reason the packing length formulation is more straightforward and more closely related to the actually measured parameters. Another parameter often used to show how much larger the chain dimensions are than those expected from an unrestricted random walk model ($R^2 = [M/m_o]l_o^2$) is the characteristic ratio, C_∞ (11). This is given by

$$C_\infty = \frac{6r_g^2 m_0}{Ml_0^2} = \frac{6m_0}{l_p l_0^2 \rho N_A} \tag{6}$$

Here l_0 is the length of the repeat unit bond (0.154 nm for C–C single bonds).

As mentioned above, successful models (2–8) have been developed to relate the entanglement molecular weight to chain dimensions. The relevant result is that M_e is proportional to ρl_p^3. The coefficient of proportionality is independent of polymer type and temperature. This has now been shown to hold for a wide range of flexible polymers, including polydienes, styrenic polymers, acrylics, and even polymeric sulfur.

$$M_e = 1.98 N_A \rho l_p^3 \tag{7}$$

If one uses ρ in units of kg/m^3, l_p in nm, and M_e in g/mol, then $M_e = 1.19\rho\, l_p^3$. Experimentally, M_e is found from the measurement of the plateau modulus through the definition of $M_e \equiv \rho RT/G_N^0$. (See Ref. 22 for a discussion of the definitions used for M_e.) Thus, for the packing length model this means that

$$G_N^0 = \frac{kT}{1.98 l_p^3} \tag{8}$$

Here k is Boltzmann's constant. With T in units of K, l_p in nm, and G_N^0 in kPa, $G_N^0 = 6.97T/l_p^3$. The utility of such a simple expression for a fundamental property like plateau modulus is clear, as I will demonstrate below.

There are several other parameters that can be used to describe the state of entanglement for flexible polymers. One of these is the volume per entanglement, V_e, which is the volume occupied by a chain of molecular weight M_e. By Eq. (1) we have

$$V_e = \frac{M_e}{\rho N_A} \tag{9}$$

Combined with Eq. (7) this gives

$$V_e = 1.98 l_p^3 \tag{10}$$

The reptation model of polymer rheology was first discussed by deGennes (23) and fully developed by Doi and Edwards (24). In this theory the restrictions on the motions of an entangled chain are modeled by confining it to a tube of diameter d_t formed by the surrounding molecules. This is defined by the relation

$$\frac{d_t^2}{M_e} = \frac{R^2}{M} \tag{11}$$

From the packing length model (6) one gets

$$d_t = l_p n_t/6 = n_t^{1/3} V_e^{1/3} \tag{12}$$

The numerical coefficient in Eq. (12), n_t, is the number of chain segments (3) of molecular weight M_e that can be found in a cube of edge length d_t. This is a constant for polyolefins (and indeed for all flexible polymers) at a value of $n_t = 20.6 \pm 1.8$.

Application to Polyolefins

Table 1 summarizes the data that exist to relate entanglements and chain dimensions for polyolefins (see Appendix for descriptions of the polymers). These are plotted in Fig. 1 as V_e vs. l_p^3. From both the table and figure, one can see that Eq. (10) and Eq. (8) works very well to describe polyolefin rheology over several orders of magnitude in plateau modulus. The quality of the fit in Fig. 1 is more impressive when one considers that these two parameters are derived from separate sets of data, l_p from SANS-derived chain dimensions, and V_e from rheology.

The success of the packing length model for explaining the degree of entanglement of a polymer can be very useful in the design of new materials. This is because the plateau modulus and M_e are the key to many of the basic performance aspects of polymers, such as processability, adhesive strength, and crystallization kinetics. For instance, this model can be used to explain the effects of tacticity on the plateau modulus of propylene polymers. The observation that syndiotactic polypropylene (s-PP) has a much higher value of G_N^0 than isotactic (i-PP) or atactic polypropylene (a-PP) was first made in 1995 (25). This is due to the significantly larger chain dimensions of s-PP (26), which is presumably due to a larger probability of *trans* over *gauche* bond rotations in s-PP as opposed to i-PP or aPP. We are now able to make a good prediction of the plateau modulus for polyolefins even before they have been synthesized, as long as we have a way to make a reasonable estimate of their chain dimensions (11). This can be a very powerful tool for modeling polymer material performance; an example is given below for adhesive performance.

Other Rheological Properties

Several other rheological properties have also been related to the packing length (7, 8). One of these is M_c, the critical molecular weight at which the zero-shear viscosity of a polymer begins to rapidly increase (generally from a linear dependence on M to a power law function, usually on the order of $M^{3.4}$) (1). An empirical fit to the data that exist on M_c (about a dozen polymers) gives

$$M_c = M_e[l_p^*/l_p]^{0.65} \tag{13}$$

In Eq. (13), l_p^* is a constant of value $\sim$6 nm. Similarly, Graessley has predicted (27) that at some large value of M, polymer viscosity should show the M^3 dependence expected from the Doi-Edwards model (24). This phenomenon has been seen for several polymers now, and this molecular weight, M_r, is given by

$$M_r = M_e[l_p^*/l_p]^{3.9} \tag{14}$$

Equations (13) and (14) can be used to estimate these technologically important critical molecular weights to model performance in, for instance, extrusion.

Table 1
Chain dimensions and rheological properties of polyolefins

Polymer	Comonomer (mol %)	m_b (g/mol)	T (K)	r_g^2/M (nm^2 mol/kg)	C_∞	ρ (kg/m^3)	l_p (nm)	b^a (nm)	G_N^0 (MPa)	M_e (kg/mol)	V_e (nm^3)	n_t	d_t (nm)
PE	—	14.0	413	2.08	7.37	784	1.02	0.77	2.60	1.04	2.19	21.18	3.59
EBR04	4	14.6	413	2.02	7.44	785	1.05	0.76	2.21	1.22	2.58	22.03	3.84
EBR09	9	15.3	413	1.92	7.41	788	1.10	0.74	1.90	1.42	3.00	22.15	4.05
EBR14	14	16.0	413	1.75	7.07	789	1.20	0.71	1.55	1.75	3.68	21.38	4.28
EBR19	19	16.7	413	1.75	7.38	791	1.20	0.71	1.40	1.94	4.07	22.58	4.51
EBR21	21	16.9	413	1.77	7.59	792	1.18	0.71	1.30	2.09	4.39	23.88	4.71
EBR23	23	17.2	413	1.59	6.93	793	1.32	0.68	1.20	2.27	4.75	21.20	4.65
alt-PEP	50	17.5	298	1.54	6.82	856	1.26	0.69	1.15	1.84	3.58	19.67	4.13
alt-PEP	50	17.5	413	1.39	6.15	790	1.51	0.63	0.95	2.86	6.00	19.37	4.88
EBR28	28	17.9	298	1.54	6.98	860	1.25	0.69	1.12	1.90	3.67	20.07	4.19
HPI-07	7	18.1	373	1.45	6.65	812	1.41	0.65	1.1	2.29	4.68	18.99	4.46
EBR35	35	18.9	298	1.54	7.36	860	1.25	0.69	1.12	1.90	3.67	20.07	4.19
EBR35	35	18.9	413	1.52	7.27	797	1.37	0.66	0.90	3.04	6.33	23.05	5.27
HPI-16	16	19.0	373	1.36	6.54	812	1.50	0.63	0.88	2.86	5.85	19.28	4.83
HPI-20	20	19.4	373	1.31	6.44	812	1.56	0.62	0.79	3.19	6.52	19.24	5.01
HPI-29	29	20.5	373	1.22	6.32	812	1.68	0.60	0.58	4.34	8.88	20.18	5.64
EBR49	49	20.9	298	1.33	7.02	864	1.44	0.64	0.69	3.10	5.96	20.66	4.98
EBR49	49	20.9	413	1.33	7.02	799	1.56	0.62	0.67	4.09	8.51	21.95	5.72
s-PP	—	21.0	463	1.72	9.14	762	1.27	0.69	1.35	2.17	4.73	22.43	4.74
alt-PEB	50	21.0	298	1.21	6.43	861	1.59	0.61	0.58	3.68	7.09	19.46	5.17
HHPP	—	21.0	298	1.15	6.11	878	1.64	0.60	0.52	4.18	7.91	19.60	5.37
a-PP	—	21.0	298	1.11	5.90	852	1.76	0.58	0.48	4.40	8.57	18.50	5.41
HHPP	—	21.0	413	1.15	6.11	810	1.78	0.58	0.52	5.35	10.96	20.45	6.08
a-PP	—	21.0	348	1.12	5.95	825	1.80	0.58	0.48	4.97	10.01	19.30	5.78
alt-PEB	50	21.0	413	1.15	6.11	800	1.80	0.58	0.52	5.28	10.96	20.07	6.04
i-PP	—	21.0	463	1.16	6.16	766	1.87	0.57	0.43	6.86	14.86	22.18	6.91

(*continued*)

Table 1
Continued

Polymer	Comonomer (mol %)	m_b (g/mol)	T (K)	r_g^2/M (nm^2 mol/kg)	C_∞	ρ (kg/m^3)	l_p (nm)	b^a (nm)	G_N^0 (MPa)	M_e (kg/mol)	V_e (nm^3)	n_t	d_t (nm)
a-PP	—	21.0	413	1.12	5.95	791	1.87	0.57	0.47	5.78	12.13	19.95	6.23
HPI-34	34	21.1	373	1.17	6.24	812	1.75	0.59	0.5	5.04	10.30	20.41	5.95
EBR64	64	23.0	298	1.07	6.22	863	1.80	0.58	0.44	4.86	9.35	18.64	5.59
EBR64	64	23.0	413	1.15	6.68	802	1.80	0.58	0.43	6.40	13.26	22.16	6.65
PI-50	50	23.3	298	1.06	6.26	861	1.82	0.57	0.35	6.10	11.75	20.53	6.23
HPI-50	50	23.3	373	1.05	6.20	812	1.95	0.56	0.35	7.19	14.71	20.74	6.73
EBR79	79	25.1	298	1.04	6.59	864	1.85	0.57	0.38	5.63	10.83	19.25	5.93
EBR79	79	25.1	413	1.08	6.85	805	1.91	0.56	0.30	9.21	19.00	24.28	7.73
EBR82	82	25.5	413	1.01	6.51	805	2.04	0.54	0.29	9.53	19.66	22.33	7.60
EBR82	82	25.5	298	0.912	5.88	864	2.11	0.53	0.30	7.14	13.71	17.79	6.25
HPDMBd-55	45	27.1	298	0.718	4.92	838	2.76	0.47	0.16	12.98	25.71	16.26	7.48
PIB	—	28.0	298	0.950	6.73	918	1.90	0.56	0.32	7.11	12.86	20.06	6.37
PIB	—	28.0	413	0.950	6.73	849	2.06	0.54	0.32	9.11	17.82	21.00	7.21
HPI-75	75	28.0	413	0.882	6.25	810	2.32	0.51	0.22	12.64	25.91	21.12	8.18
a-PB	—	28.0	298	0.808	5.72	866	2.37	0.50	0.18	11.92	22.85	19.22	7.60
a-PB	—	28.0	413	0.845	5.99	807	2.43	0.50	0.20	13.86	28.51	20.65	8.38
HPI-75	75	28.0	298	0.773	5.48	878	2.45	0.50	0.19	11.45	21.65	17.87	7.29
HPI-75	75	28.0	373	0.827	5.86	812	2.47	0.49	0.2	12.59	25.75	19.18	7.90
s-PPEN	—	35.0	303	0.930	8.23	850	2.10	0.53	0.2	10.71	20.91	22.08	7.73
HPMyrc-03	3	35.5	298	0.723	6.50	853	2.69	0.47	0.14	15.10	29.38	18.04	8.09
i-PHEX	—	42.0	273	0.927	9.85	872	2.05	0.54	0.14	14.14	26.92	25.90	8.87
s-PHEX	—	42.0	273	0.785	8.34	872	2.43	0.50	0.13	15.23	28.99	20.95	8.47
PCHE	—	42.0	413	0.538	5.72	920	3.35	0.42	0.07	46.46	83.84	21.90	12.25
HPMyrc-36	36	42.7	298	0.682	7.36	849	2.87	0.46	0.10	21.04	41.14	19.41	9.28
s-POCT	—	56.0	273	0.655	9.28	872	2.91	0.45	0.0757	26.15	49.78	20.92	10.14

[a]Statistical segment length (Eq. (5)) with reference volume $v_0 = 0.1\,nm^3$.

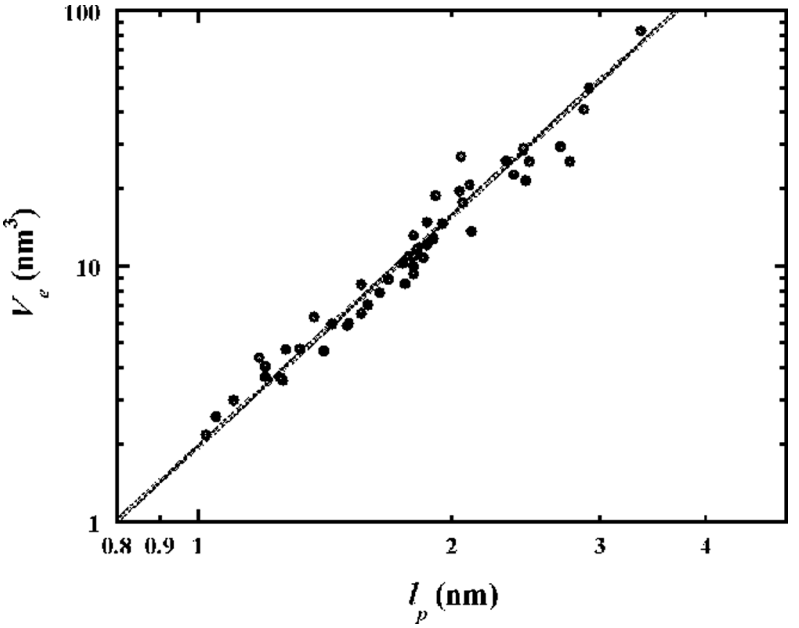

Figure 1. Plot of V_e vs. l_p^3 for polyolefins. Solid line is from Eq. (10).

The degree of entanglement, as represented by M_e or G_N^0, is one of two basic parameters that is critical to modeling polymer rheology. The other one is a measure of the basic process involved in moving one monomer repeat unit past another (1, 24). This can be represented by a so-called friction factor, ζ, or an equilibration time, τ_e. One can use the values of M_e and ζ for a polymer and predict the rheological performance of a linear sample just from a knowledge of the molecular weight distribution (28, 29). Unfortunately, there is only a small amount of data for friction factors on polyolefins from rheology (30–33) or diffusion experiments (34). As of this date there has been no correlation of these values with the chemical structure of the polymers, unlike the case for plateau modulus or entanglement density. As more data are recorded, developing such relationships will become more likely, and will clearly be a focus of research. Until such understanding is developed, one will need to rely on the few published values or on directly measured numbers for friction factor to further the use of these models.

Miscibility

The wealth of data on polyolefin blends generated over the last several years has been compiled in a number of reviews (35, 36). One of the most interesting features of polyolefin miscibility that has been discovered in this work is the great range of phase behavior shown by these systems. Most polyolefin blends display UCST (upper critical solution temperature) phase diagrams with phase separation occurring upon cooling, but many are characterized by LCST (lower critical solution temperature) behavior by phase separating when heated. Some show both an LCST and a UCST. This great diversity in phase behavior may be regarded as surprising from saturated hydrocarbon polymers that interact only through dispersive, van der Waals forces.

The second interesting feature is that the great majority of these data can be explained by regular solution theory (37). That is, interaction energy densities for most of these blends can be determined from the square of the difference between the solubility parameters of the two components, and that these solubility parameters are simply the square roots of the cohesive energy densities of the pure polymers. This is not universally true for polyolefin blends, and in fact several blends, especially those involving polyisobutylene (38), show negative values of the interaction energy density. As a general rule, we have seen that regular solution theory nearly always explains the miscibility of two saturated hydrocarbon polymers when one or both components are copolymers, but only rarely does so for mixtures of two homopolymers. Regular solution theory does describe the miscibility data of around 80% of the blends that we have studied so far, and since almost all blends involve at least one copolymer, it should work for nearly all blends of commercial interest. Moreover, for most of the irregular blends the difference of the data from the regular solution predictions can be used to characterize the anomalies (39). So an understanding of the origins of polyolefin solubility parameters provides a foundation for understanding polyolefin miscibility.

As mentioned above, a large number of polyolefin solubility parameters have now been compiled (35). Some of these values are shown in Table 2. These are polyolefins for which we have direct measures of density, melt chain dimensions (10), and solubility parameters derived from interaction energies measured on polyolefin blends by small angle neutron scattering. A significant hurdle in developing the solubility parameter model of polyolefin miscibility is that the cohesive energies of the polymers cannot be directly measured (see below) (37). However, the solubility parameter values in Table 2

Table 2
Polyolefin solubility parameters, δ, in units of $MPa^{1/2}$

	T (°C)				
Polymer	27	51	83	121	167
HPI-75	18.00	17.59	16.91	16.53	15.70
EB97	18.17	17.76	17.08	16.69	15.86
EB88	18.40	17.98	17.29	16.89	16.04
a-PP	18.39	17.98	17.33	16.95	16.11
EB78	18.66	18.24	17.54	17.13	16.27
HPI-50	18.68	18.26	17.56	17.14	16.29
EB66	18.90	18.48	17.77	17.35	16.48
alt-PEB	18.89	18.48	17.79	17.38	16.52
HHPP	18.99	18.55	17.84	17.41	16.53
EB52	19.18	18.74	18.03	17.60	16.72
alt-PEP	19.09	18.67	17.98	17.58	16.74
EB38		18.96	18.24	17.80	16.91
EB35		18.98	18.25	17.82	16.93
EB32		19.10	18.36	17.91	17.01
EB25			18.45	18.00	17.09
EB17				18.06	17.16
EB08				18.23	17.29

have been corroborated by measurements of the internal pressure of pure polyolefin components, which have been determined by the response of the polymer density to temperature and pressure (*PVT* data). The reader is directed to reference 35 for a fuller discussion of the relation of internal pressure to cohesive energy density, but it is worthwhile to point out that this relation for polyolefins is very similar to that seen for low molecular weight alkanes (40) for which both cohesive energy density and internal pressure can be directly measured. There is thus a great deal of confidence in these numbers, and as will be shown below, they can be used to predict the miscibility of polyolefin blends quite well.

It is well known that a chief distinguishing feature of polymer blends is that the entropy of mixing is very small, due to the large size of macromolecules (41). This can be seen in the Flory-Huggins-Staverman (42–44) expression for the free energy of mixing:

$$\Delta G_m = RT\left\{\frac{\phi_1\rho_1}{M_1}\ln\phi_1 + \frac{\phi_2\rho_2}{M_2}\ln\phi_2\right\} + X_{12}\phi_1\phi_2 \tag{15}$$

In Eq. (15), R is the gas constant, ρ_i is the density of polymer i, ϕ_i is the volume fraction of component i, and X_{12} is the interaction energy density between the two polymers. The interaction energy density is directly related to the more commonly used Flory interaction parameter, χ_{12}, by the relation:

$$X_{12} = \frac{\chi_{12}}{v_0}RT \tag{16}$$

where v_0 is a reference volume to normalize the value of χ_{12}. When comparing the interactions for many different blends, the choice of v_0 becomes arbitrary, as it is for the statistical segment length (Eq. (5)). So herein the interaction energy density formulation of Eq. (15) will be used.

The power of regular solution theory is that it provides a way to predict miscibility in blends from parameters that are determined for the individual components. This basic parameter is the so-called solubility parameter for polymer i, δ_i, which is just the square root of the cohesive energy density of the polymer (37). The cohesive energy is that which holds the molecules of a substance together in the condensed (liquid) state, and so is given by the heat of vaporization (40). Obviously, this cannot be directly determined for most polymers, since they degrade at temperatures well below those at which they would boil. But one can get reasonable estimates of δ_i from *PVT* measurements and values can also be derived by redundancy from a large set of values for X_{12} when the number of blends is significantly greater than the number of component polymers (35). One caution for the reader is that values of δ_i from group contribution schemes do not work for polyolefins, as explained in reference 35.

Given the values of solubility parameters, it is quite simple to estimate the interaction energy density, since:

$$X_{12} = (\delta_1 - \delta_2)^2 \tag{17}$$

On the other hand, by measuring X_{12} for many pairs of polymers, one can extract values of δ_i for the components, given the value for just one of them. (Herein, the reference value is taken to be that for atactic polybutene, determined from *PVT* evaluation of internal pressure.) Such an assignment becomes more well founded the greater the number of blends measured, and the greater the redundancy of assigning solubility parameters. The values for the 17 polymers in Table 2 come from measuring X_{12} for 42 blends over

a range of temperatures. Note that the derivation of δ's from X_{12} needs to be performed at each temperature separately. Cohesive energy density, and so δ, generally decreases as T increases, but at different rates for each polymer. Thus, even under regular solution theory, all kinds of phase behavior (LCST and UCST) can be seen.

In Fig. 2, the values of δ/ρ are plotted vs. l_p, showing that there is a clear correlation of solubility parameter with chain dimensions, as reported by several authors (35, 45). To enable the prediction of miscibility, the question then arises as to how to translate this observation into a formula for determining δ directly from data or calculations of chain dimensions. It has recently been shown (18) that a reasonable answer can be found in the PRISM theory of Schwiezer and Singh (17). This is based on a theory of liquids that has been successfully applied to many polymer problems. A quite simple expression for the dependence of δ on temperature and chain dimensions comes from this model:

$$\delta = \frac{\rho N_A}{m_0}\left[\frac{2\pi\varepsilon a^3}{\left(1+(l_p/2\pi a)\right)}\right]^{1/2} \tag{18}$$

In Eq. (18), a and ε are parameters that represent the length and energy scales of the interactions between the polymers. Fitting the values in Table 2, we find that $a = 0.80$ nm and $\varepsilon = 6.53 \times 10^{-4}$ eV, or $\varepsilon/k = 7.6$ K (taking $m_0 = 14$ g/mol for a methylene unit), which are reasonable values for the van der Waals potential typical of polyolefin blends. The power of Eq. (18) is that it allows the prediction of polyolefin miscibility from simply knowing chain dimensions, as will be demonstrated in the last section.

Models of Chain Dimensions

Equations (8) and (18) give us powerful tools to allow the prediction of some basic physical properties of polyolefin melts (i.e., their degree of entanglement and their miscibility with other polyolefins) if we know the dimensions of the chains that comprise these materials. While many of these dimensions are known (see Table 1), this predictive power becomes all the more useful if ways to estimate the sizes of polyolefin molecules can be found, especially for those that have not yet been synthesized. Direct measurement of melt chain dimensions by neutron scattering (10) is the surest way to such data, but this generally

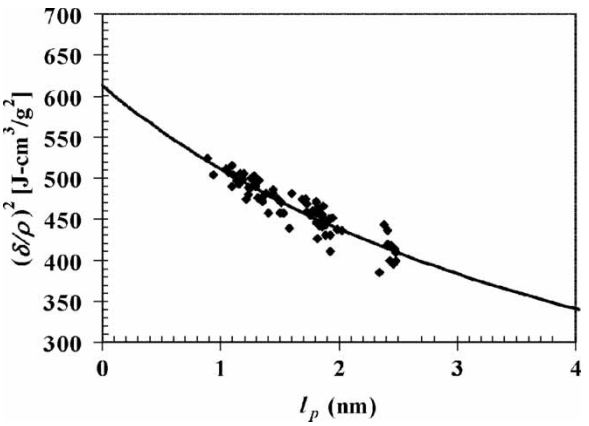

Figure 2. Plot of δ vs. l_p for polyolefins. Solid line is Eq. (18) with $a = 0.80$ nm and $\varepsilon/k = 7.6$ K.

requires access to deuterated polymers and a neutron source. Estimates of the bulk melt dimensions are sometimes possible from dilute solution, theta-state values, but this only gives a qualitative idea of chain size, and not a numerical value (6). One method that often works to calculate polymer dimensions from first principles is the rotational isomeric state model (11), but for many polyolefins this has given results at odds with experiment (6). A promising new correlation of polyolefin chain dimensions with chemical structure has recently been found, and this is described in the rest of this section.

This correlation comes from an observation of how the dimensions of chains depend on a simple feature of the chemical architecture, which is m_b, the molecular weight per backbone bond (46). In Fig. 3, l_p is plotted *vs.* m_b at 190°C. While there is not yet a clear physical model for these relations, it has been found that the dimensions of most polyolefin chains obey the following relations with m_b at 190°C (for l_p in units of nm):

$$l_p = 0.0333 m_b^{1.30} \qquad 14 \text{ g/mol} < m_b < 28 \text{ g/mol} \tag{19a}$$

$$l_p = 0.627 m_b^{0.42} \qquad m_b > 28 \text{ g/mol} \tag{19b}$$

Of course, the values of l_p depend on temperature, but this dependence is fairly small and of secondary importance to that on m_b. Moreover, the temperature dependence of l_p is quite similar for most polyolefins, so the relative rankings are fairly consistent at all temperatures. Therefore Eq. (19) satisfies the main objective of a reasonable estimate of entanglement and miscibility attributes. It is clear from Fig. 3 that the relations in Eq. (19) work quite well for most cases. The clearest outlier is s-PP, followed by PIB.

As explained in reference 46, the variation of l_p with m_b is mostly due to changes in the "thickness" of the chain (i.e., how much of the chain is in the side branches instead of in the backbone), but also is partly a result of differences in chain stiffness (i.e., the tendency for *trans* vs. *gauche* rotations). A good way to separate out the effects of stiffness is to look at how C_∞ depends on m_b. This is shown in Fig. 4, and from Eqs. (6) and (19) we have, at 190 °C:

$$C_\infty = 16.1 m_b^{-0.30} \qquad 14 \text{ g/mol} < m_b < 28 \text{ g/mol} \tag{20a}$$

$$C_\infty = 0.859 m_b^{0.58} \qquad m_b > 28 \text{ g/mol} \tag{20b}$$

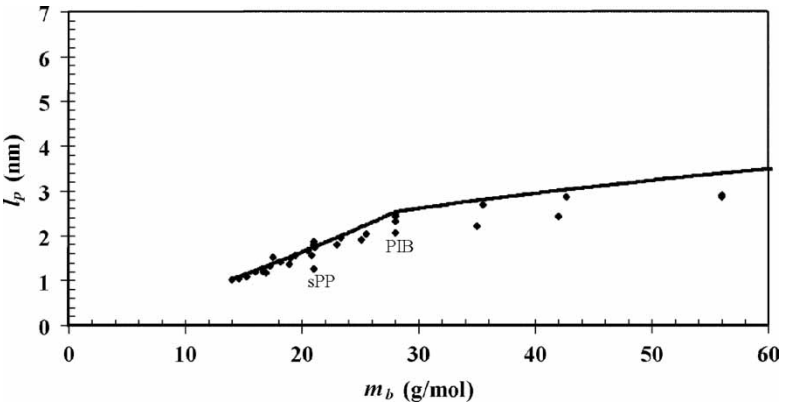

Figure 3. Dependence of l_p on m_b at 190°C. Solid line is from Eq. (19).

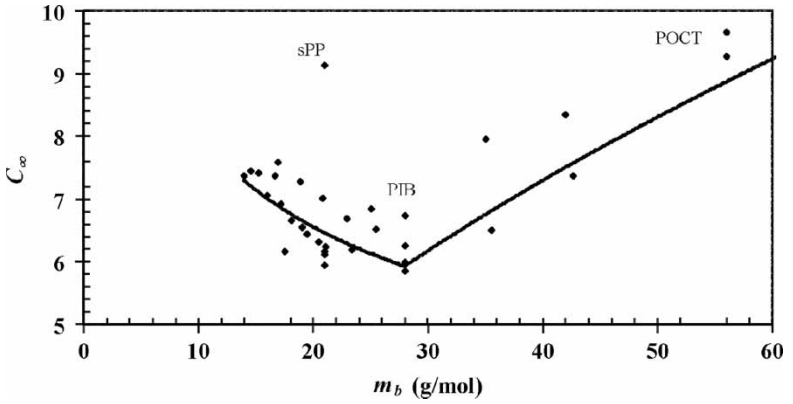

Figure 4. Dependence of C_∞ on m_b at 190°C. Solid line is from Eq. (20).

Another representation of this is to plot C_∞ vs. f, the fraction of carbons that are in the backbone. For polyolefins f is given by $14/m_b$. This gives the corresponding dependence of C_∞ depends on f, which is shown in Fig. 5:

$$C_\infty = 7.29 f^{0.30} \qquad 0.5 < f < 1.0 \tag{21a}$$

$$C_\infty = 4.14 f^{-0.58} \qquad f < 0.5 \tag{21b}$$

In Fig. 5, one can see that C_∞ reaches a minimum of about 5.9 at $f = 1/2$, that is, when half of the polymer is in the backbone and half is in the branches. This applies to both atactic polybutene, with an ethyl branch for every two backbone carbons, and an ethylene-octene copolymer with 33 mol% octene, with a hexyl branch for every six backbone carbons. One might speculate that this is the point at which the presence of the branches is most effective at changing the bond rotations of the backbone, that is, at increasing the proportion of *gauche* rotations. For $f > 1/2$, there are significant long stretches of methylene segments that will favor *trans* rotations. For $f < 1/2$, the branches are longer than the spacings between them, and so the chain cannot twist enough to avoid

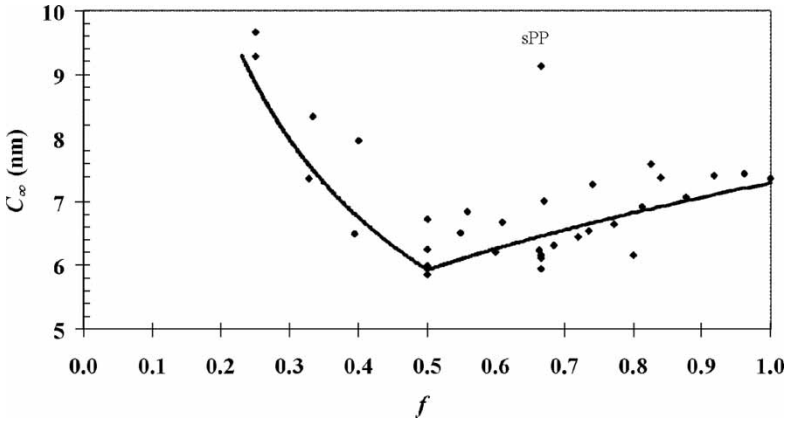

Figure 5. Dependence of C_∞ on f at 190°C. Solid line is from Eq. (21).

eclipsing of the branches with each other. However, it would be good to put this empirical observation on a firmer foundation of understanding. Moreover, it is important to point out the exceptions to this rule, such as sPP and PIB, as the utility of such materials depends on their special values of chain dimensions. However, the relations shown in Eqs. (19), (20), and (21) can be used to give a rough estimate of the dimensions of most polyolefins, and so an estimate of their melt properties. Some examples of these predictions are given in the next section.

Predictions

Plateau Modulus

The applications where a particular polymer will be useful depend to a large degree on its plateau modulus. For example, the tensile modulus of crosslinked elastomers depends not only on the level of curing that is present, but also on the entanglements that are trapped by the chemical crosslinks (47). For this reason, ethylene-propylene elastomers have a higher level of tensile strength than other rubbers (see ref. 47, Fig. 24, and Table 8). On the other hand, for adhesive applications, a low plateau modulus is desired, as captured in the well-known Dahlquist criterion (48). The low modulus is needed to ensure that the adhesive will flow over all of the asperities on a surface and so provide a large bonding area and good adhesion. So there is a need to provide polyolefins with a wide range of plateau modulus, and to show how this is controlled by chemical architecture.

An example is given in Fig. 6, where the predictions of Eqs. (8) and (19) for the plateau moduli of ethylene- and propylene-copolymers are shown. For the available data, these descriptions work well (as discussed above), but most of the copolymers indicated in the figure have never been made. As a class, it is clear that propylene copolymers have a much lower plateau modulus than ethylene copolymers. The influence of the amount and length of the short braches is also apparent. The Dahlquist criterion is also shown in Fig. 6, showing where one might expect good adhesive behavior. It is clear

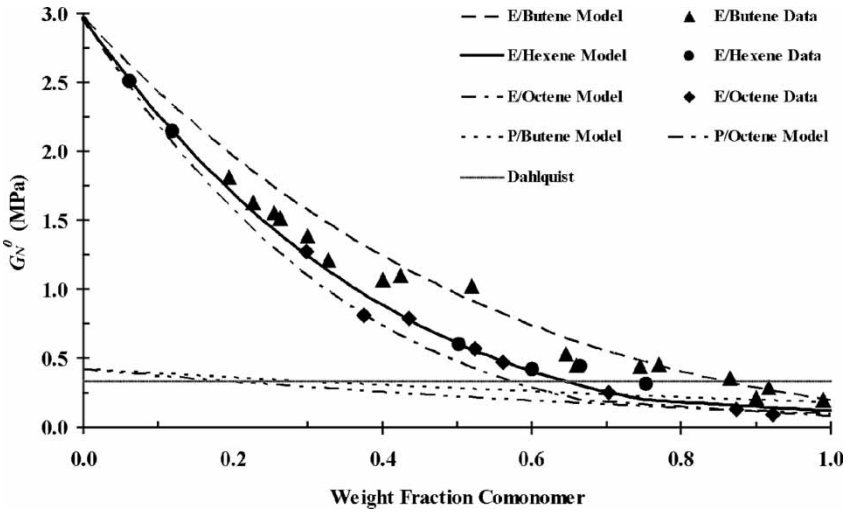

Figure 6. Plateau moduli of ethylene and propylene copolymers.

how the kind of information contained in Eqs. (8) and (19), and Fig. 6, can be used to define promising areas in which to explore new product opportunities that depend on rheological performance.

Miscibility

The solubility parameters of polyolefins can be estimated from Eqs. (18) and (19) in a very direct way. For instance, the variation in δ with comonomer content can be derived for various ethylene copolymers. This is shown in Fig. 7 for $T = 167^{\circ}\mathrm{C}$. There is a regular drop in δ as the amount and length of the short chain branches increase. (Note that such a dependence of solubility parameter on comonomer could never be predicted by any group contribution scheme.) As mentioned above, these relations are well founded on neutron scattering and *PVT* measurements (35). The predictions of Eqs. (18) and (19) as seen in the curves in Fig. 7 can be used to predict the miscibility of blends for which there are no direct data on the thermodynamics. For example, these relationships explain very well the miscibility behavior shown by various ethylene-octene copolymers with each other (49).

We can also use it to understand which ethylene copolymers will be miscible with polypropylene (50). This can be seen in Fig. 8, where scanning electron micrographs of blends of several ethylene copolymers with polypropylene are shown. All of the blends were 80 wt% PP and 20 wt% of the copolymers. The copolymers have been extracted with hexane to produce these samples, so the holes seen are where the copolymer used to be. For the two ethylene-propylene copolymers, it is perhaps not surprising that the 90 wt% propylene EP is miscible with PP while the one at 54 wt% is not. However, it is revealing that this situation is reversed for ethylene-octene copolymers, as can be seen in Fig. 8c and 8d. This surprising result is a direct consequence of chain dimensions of the copolymers, and how they compare with PP. It can be reconciled using Fig. 7, where the predicted solubility parameters for the four copolymers shown in Fig. 8 are indicated by the four boxes. The shaded box marked "miscibility region" shows the range of solubility parameters for polymers to mix regularly with polypropylene when both components have $M_w = 100\,\mathrm{kg/mol}$ (at 167°C). The blends with the two copolymers

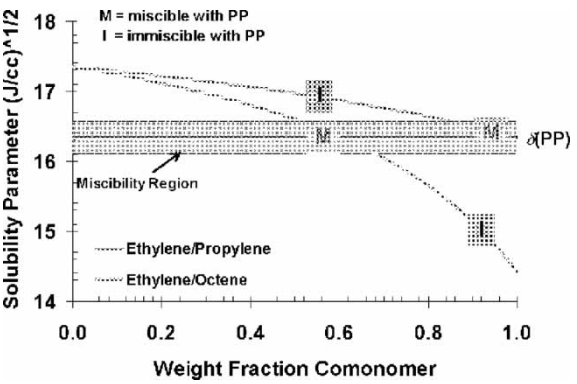

Figure 7. Solubility parameters of ethylene copolymers at 167°C. The four boxes correspond to the four copolymers in Fig. 8.

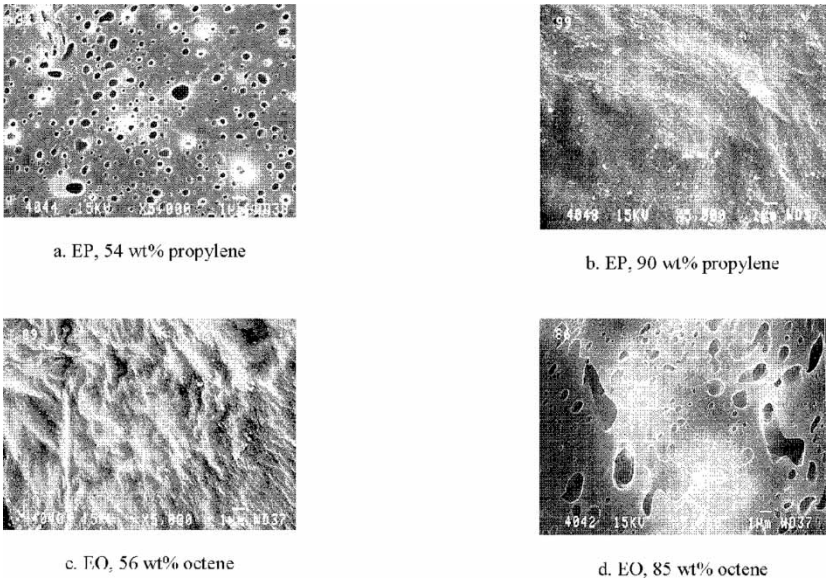

Figure 8. SEM micrographs of 80/20 PP/copolymer blends. Samples were extracted with hexane at room temperature to reveal location of soluble copolymer domains.

that were predicted to fall into this miscibility region (the 90 wt% propylene EP and the 56 wt% octene EO) did indeed show a single-phase morphology, while the other two mixtures were clearly immiscible. There is thus a good correlation of the predictions with experimental miscibility. Again, let me caution that this model will not predict *all* of polyolefin miscibility, and that the behavior of some important systems such as polyisobutylene blends is irregular (38). However, the great majority of polyolefin blends obey these relations, and this simple scheme gives us a very good way to begin to estimate the thermodynamics of these important materials.

Future Areas of Work

In this paper I have shown how we now have some basic understanding of the way two of the most important parameters that determine the properties of polyolefins, the degree of entanglement and mutual solubility, are related to the chemical nature of the chains. This understanding has translated into some highly useful tools for designing new materials based on either existing or novel polyolefins. The fact that we have found success for G_N^0 and X_{12} should give one confidence that a similar degree of understanding can also be achieved for other basic properties. It is known that some mechanical properties, such as yield stress (51) and tensile performance (52) can be related to entanglement. We might also hope to relate other basic properties, such as glass transition temperature, monomeric friction factor, crystallization kinetics, and crystal structure back to the chemistry of the chains. If this can indeed be done for polyolefins, then such work could serve as a model for doing so for polymers in general. I believe that the results outlined herein represent just the first step toward realization of Paul Flory's dream of directly relating the performance of polymeric materials back to the configurations of

the chains from which they are made. But they do show that such a path can be traveled and point the way to the next steps.

Appendix

Name	Description
alt-PEB	essentially alternating poly(ethylene-co-1-butene)
alt-PEP	essentially alternating poly(ethylene-co-propylene)
a-PB	atactic poly(butene-1)
a-PDEC	atactic poly(decene-1)
a-PHDEC	atactic poly(hexadecene-1)
a-PHEX	atactic poly(hexene-1)
a-POCT	atactic poly(octene-1)
a-PP	atactic polypropylene
a-PPEN	atactic poly(pentene-1)
EBRx	ethylene-butene random copolymer with x mole percent butene incorporation
EHRx	ethylene-hexene random copolymer with x mole percent hexene incorporation
EODRx	ethylene-octadecene random copolymer with x mole percent octadecene incorporation
EORx	ethylene-octene random copolymer with x mole percent hexene incorporation
EPRx	ethylene-propylene random copolymer with x mole percent propylene incorporation
HHPP	head-to-head polypropylene; HPDMBd-100
HPDMBd-x	hydrogenated poly(dimethyl butadiene) containing x% 1,4 units
HPI-x	hydrogenated polyisoprene, x = 3,4 content of parent polyisoprene
HPMyrc-x	hydrogenated poly(myrcene) with x% 3,4
i-PHDEC	isotactic poly(hexadecene-1)
i-PHEX	isotactic poly(hexene-1)
i-PPEN	isotactic poly(pentene-1)
PCHE	atactic poly(cyclohexylethylene); via the hydrogenation of polystyrene
PE	polyethylene
PIB	polyisobutylene
PPT	poly(pentenamer)
s-PHEX	syndiotactic poly(hexene-1)
s-POCT	syndiotactic poly(octene-1)
s-PPEN	syndiotactic poly(pentene-1)

Acknowledgments

As can be seen from the list of references, the results described in this paper have come from collaborations with many coworkers, both inside and outside of ExxonMobil. Chief among these are Bill Graessley, Nikos Hadjichristidis, Lew Fetters, and César García-Franco, whom I want to especially thank. I am also grateful to Bryan Chapman for useful suggestions on this manuscript.

References

1. Ferry, J.D. (1980) *Viscoelastic Properties of Polymers*, 3rd Ed.; John Wiley and Sons: New York, 482 pp.
2. Ronca, G.J. (1983) Frequency Spectrum and Dynamic Correlations of Concentrated Polymer Liquids. *J. Chem. Phys.*, 79 (2): 1031–1043.
3. Lin, Y.H. (1987) Number of Entanglement Strands per Cubed Tube Diameter, a Fundamental Aspect of Topological Universality in Polymer Viscoelasticity. *Macromolecules*, 20 (12): 3080–3083.
4. Kavassalis, T.A. and Noolandi, J. (1987) New View of Entanglements in Dense Polymer Systems. *Phys. Rev. Lett.*, 59 (23): 2674–2677.
5. Colby, R.H. and Rubinstein, M. (1990) Two-Parameter Scaling for Polymers in Θ Solvents. *Macromolecules*, 23 (10): 2753–2757.
6. Fetters, L.J., Lohse, D.J., Richter, D., Witten, T.A., and Zirkel, A. (1994) The Connection Between Polymer Chain Packing Length and Melt Viscoelastic Properties. *Macromolecules*, 27 (17): 4639–4647.
7. Fetters, L.J., Lohse, D.J., and Graessley, W.W. (1999) Chain Dimensions and Entanglement Spacings in Dense Macromolecular Systems. *J. Polymer Science—Physics*, 37: 1023–1033.
8. Fetters, L.J., Lohse, D.J., Milner, S.T., and Graessley, W.W. (1999) Packing Length Influence in Linear Polymer Melts on the Entanglement, Critical, and Reptation Molecular Weights. *Macromolecules*, 32 (20): 6847–6851.
9. Rubin, R.J. (1972) Span of a Polymer Chain. *J. Chem. Phys.*, 56 (12): 5747–5757.
10. Wignall, G.D. (1987) Neutron Scattering. *Encyclopedia of Polymer Science and Engineering*. Wiley: New York, 112–184.
11. Flory, P.J. (1969) *Statistical Mechanics of Chain Molecules*. Interscience: New York, 432.
12. Lohse, D.J. (2000) Polyolefins. In *Applied Polymer Science—21st Century*. Craver, C.D. and Carraher, C.E., Eds.; Elsevier: Amsterdam, 73–91, ch. 6.
13. Rachapudy, H., Smith, G.G., Raju, V.R., and Graessley, W.W. (1979) *J. Polym. Sci.—Physics*, 17: 1211.
14. Hadjichristidis, N. et al. (2000) Well-Defined, Model Long Chain Branched Polyethylene: Part 1: Synthesis and Characterization. *Macromolecules*, 33 (7): 2424–2436.
15. Hamielec, A.E. and Soares, J.B.P. (1996) Polymerization Reaction Engineering—Metallocene Catalysts. *Prog. Polym. Sci.*, 21 (4): 651–706.
16. Smith, J.A., Brzezinska, K.R., Valenti, D.J., and Wagener, K.B. (2000) Precisely Controlled Methyl Branching in Polyethylene via Acyclic Diene Metathesis (ADMET) Polymerization. *Macromolecules*, 33 (10): 3781–3794.
17. Schweizer, K.S. and Singh, C. (1995) Microscopic Solubility-Parameter Theory of Polymer Blends: General Predictions. *Macromolecules*, 28 (6): 2063–2080.
18. Lohse, D.J. (in press).
19. Witten, T.A., Milner, S.T., and Wang, Z.-G. (1989 In *Multiphase Macromolecular Systems*; Culbertson, B.M. Eds.; Plenum: New York.
20. Helfand, E. and Sapse, A.M. (1975) Theory of Unsymmetric Polymer–Polymer Interfaces. *J. Chem. Phys.*, 62 (4): 1327–1331.
21. Graessley, W.W. (2004) *Polymeric Liquids and Networks: Structure and Properties*. Garland Science: New York, Ch. 4, pp. 559, p. 136.
22. Larson, R.G., , T., Leal, G.H., McKinley, A.E., Likhtman, A.E., and McLeish, T.C.B. (2003) Definitions of Entanglement Spacing and Time Constants in the Tube Model. *J. Rheol.*, 47 (3): 809–818.
23. de Gennes, P.-G. (1974) *J. de Physique Lettres*, 35 (4): L-133–L-135.
24. Doi., M. and Edwards, S.F. (1986) *The Theory of Polymer Dynamics*. Clarendon: Oxford, 391.
25. (a) Wheat, W.R. *ANTEC Proceedings*, 1995, 2275–2278; (b) Eckstein, A., Suhm, J., Friedrich, C., Maier, R.-D., Sassmannhausen, J., Bochmann, M., and Mülhaupt, R. (1998) Determination of Plateau Moduli and Entanglement Molecular Weights of Isotactic, Syndiotactic, and

Atactic Polypropylenes Synthesized with Metallocene Catalysts. *Macromolecules*, 31 (4): 1335–1340.
26. Jones, T.D. et al. (2002) Effect of Tacticity on Coil Dimensions and Thermodynamic Properties of Polypropylene. *Macromolecules*, 35 (13): 5061–5068.
27. Graessley, W.W. (1982) Entangled Linear, Branched, and Network Polymer Systems—Molecular Theories. *Adv. Polymer Sci.*, 47: 67–117.
28. Wasserman, S.H. and Graessley, W.W. (1996) Prediction of Linear Viscoelastic Response for Entangled Polyolefin Melts from Molecular Weight Distribution. *Polym. Engg. And Sci.*, 36 (6): 852–861.
29. Likhtman, A.E. and McLeish, T.C.B. (2002) Quantitative Theory for Linear Dynamics of Linear Entangled Polymers. *Macromolecules*, 35 (16): 6332–6343.
30. Pattamaprom, C. and Larson, R.G. (2001) Predicting the Linear Viscoelastic Properties of Monodisperse and Polydisperse Polystyrenes and Polyethylenes. *Rheol. Acta*, 40 (6): 516–532.
31. Vega, D.A., Sebastian, J.M., Russel, W.B., and Register, R.A. (2002) Viscoelastic Properties of Entangled Star Polymer Melts: Comparison of Theory and Experiment. *Macromolecules*, 35 (1): 169–177.
32. Pryke, A., Blackwell, R.J., McLeish, T.C.B., and Young, R.N. (2002) Synthesis, Hydrogenation, and Rheology of 1,2-Polybutadiene Star Polymers. *Macromolecules*, 35 (2): 467–472.
33. van Meerwald, J. (2004) A Method to Extract the Monomer Friction Coefficient from the Linear Viscoelastic Behavior of Linear, Entangled Polymer Melts. *Rheol. Acta*, 43 (6): 615–623.
34. Scheffold, F., Eiser, E., Budkowski, A., Steiner, U., Klein, J., and Fetters, L.J. (1996) Surface Phase Behavior in Binary Polymer Mixtures. I. Miscibility, Phase Coexistence, and Interactions in Polyolefin Blends. *J. Chem. Phys.*, 104 (21): 8786–8794.
35. Thermodynamics of Polyolefin Blends; Lohse, D.J. and Graessley, W.W.; vol. 1, ch. 8, pp. 219–237, Polymer Blends: Formulation and Performance, ed. by Paul, D.R. and Bucknall, C.B., Wiley: New York, 2000, 1190 pp.
36. Crist, B. and Hill, M.J. (1997) Recent Developments in Phase Separation of Polyolefin Melt Blends. *J. Polym. Sci.—Phys.*, 35 (14): 2329–2353.
37. Hildebrand, J.H. and Scott, R.L. (1950) *The Solubility of Non-Electrolytes*, 3rd Edition; Van Nostrand-Reinhold: Princeton; reprinted Dover Press, New York, 1964, 376.
38. Krishnamoorti, R., Graessley, W.W., Fetters, L.J., Garner, R.T., and Lohse, D.J. (1995) Anomalous Mixing Behavior of Polyisobutylene with Polyolefins. *Macromolecules*, 28 (4): 1252–1259.
39. Reichart, G.C., Graessley, W.W., Register, R.A., Krishnamoorti, R., and Lohse, D.J. (1997) Anomalous Attractive Interactions in Polypropylene Blends. *Macromolecules*, 30 (10): 3036–3041.
40. Allen, G., Gee, G., and Wilson, G.J. (1960) Intermolecular Forces and Chain Flexibilities in Polymers: I. Internal Pressures and Cohesive Energy Densities of Simple Liquids. *Polymer*, 1: 456–466.
41. Paul, D.R. and Bucknall, C.B. eds. (2000) *Polymer Blends: Formulation and Performance*. Wiley: New York, 1190.
42. Huggins, M.L. (1941) Solutions of Long Chain Compounds. *J. Chem. Phys.*, 9 (5): 440.
43. Flory, P.J. (1941) Thermodynamics of High Polymer Solutions. *J. Chem. Phys.*, 9 (8): 660–662.
44. Staverman, A.J. (1941) The Entropy of Liquid Mixtures. II. Deviations from Raoult's Law in Mixtures Containing Large, Flexible Molecules. *Recl. Trav. Chim.*, 60: 640–649.
45. Bates, F.S. and Fredrickson, G.H. (1994) Conformational Asymmetry and Polymer-Polymer Thermodynamics. *Macromolecules*, 27 (4): 1065–1067.
46. Fetters, L.J., Lohse, D.J., García-Franco, C.A., Brant, P., and Richter, D. (2002) Prediction of Melt State Polyolefin Rheological Properties: The Unsuspected Role of the Average Molecular Weight per Backbone Bond. *Macromolecules*, 35 (27): 10096–10101.
47. VerStrate, G. and Lohse, D.J. (1994) Structure Characterization on the Science and Technology of Elastomers. In: Mark, J.E., Erman, B. and Eirich, F.R. eds. Chapter 3 in Science and Technology of Rubber. Academic Press: New York, 95–188.

48. Dahlquist, C.A. (1959) *Adhesives Age*, 2 (10): 25–29.
49. Bensason, S., Nazarenko, S., Chum, S., Hiltner, A., and Baer, E. (1997) Blends of Homogeneous Ethylene-Octene Copolymers. *Polymer*, 38 (14): 3513–3520.
50. Yamaguchi, M., Miyata, H., and Nitta, K.-H. (1996) Compatibility of Binary Blends of Polypropylene with Ethylene-α-olefin Copolymer. *J. Appl. Polym. Sci.*, 62 (1): 87–97.
51. Ho, J., Govaert, L., and Utz, M. (2003) Plastic Deformation of Glassy Polymers: Correlation between Shear Activation Volume and Entanglement Density. *Macromolecules*, 36 (19): 7398–7404.
52. Hiss, R., Hobeika, S., Lynn, C., and Strobl, G. (1999) Network Stretching, Slip Processes, and Fragmentation of Crystallites during Uniaxial Drawing of Polyethylene and Related Copolymers. A Comparative Study. *Macromolecules*, 32 (13): 4390–4403.